Effect of Beam-to-Column Connection Details on Deformation Capacity of Cyclic Loading

K.Takatsuka, K.Suita & Y.Manabe
Kyoto University, Japan

T.Tanaka & T.Tsukada
Kobe University, Japan

SUMMARY:
This paper presents results of full-scale cyclic loading tests under constant deformation amplitude conducted to evaluate deformation capacity of welded beam-to-column connection adopted in a moment frame. Test specimens are designed and fabricated to investigate the effect of the weld access hole on deformation capacity. The relationships between ductility amplitude of loading and cumulative plastic deformation is revealed from test results. The relationships between crack propagation at welded joint and strength of connection is evaluated regarding connection details and deformation amplitude.

Keywords : Steel structure, Welded moment connection, Deformation capacity, Crack propagation

1. INTRODUCTION

Since long-period ground motions have long duration and cause large number of repeated plastic response, not only the maximum deformation but also the repeated plastic deformation significantly effect on the deformation capacity of steel frame (Suita,2007~2009). The objective of this study is to evaluate the deformation capacity of steel moment connections under repeated plastic deformation. And this paper presents the effect of weld access hole of beam-to-column connection on fracture behavior and deformation capacity. A number of studies about the effect of weld access hole were done in Japan by Inoue (1997), et al and in USA by Miller (1998), et al and summarized in FEMA, which revealed stress concentration at the toe of the weld access hole and would early fracture caused by this concentration. But a few studies about cyclic loading tests under constant deformation amplitude was done by Nakagomi (1994), Kuwamura (2004) and Iyama (2009), which could reveal deformation capacity for the low cycle fatigue.

This paper presents the result of cyclic loading tests under constant deformation amplitude conducted to investigate deformation capacity of SN490 steel beam-to-column connection. Especially, this paper focuses on the crack propagations at the toe of the weld access hole and at the end of CJP weld lines, analyzes the relationship with deformation capacity and studies quantitatively effect of connection details on deformation capacity.

2. REPEATED LOADING TEST

2.1. Test Specimen

A total of 28 steel beam-to-column subassemblages were prepared for loading tests as shown in Fig. 2.1 and 2.2. All specimens consisted of a cold-formed square tube column and a rolled wide-flange beam, and these were connected by diaphragm referred to as the through-diaphragm connection, and complete joint penetration groove welds were used to connect the beam flanges to the diaphragm plate.

Major parameters of tests are as follows and summarized in Table 2.1.

(1)The beam end connection of SCS and SC series were constructed using weld access hole detail (WAH type), while that of NSS, NSW and NS series were constructed using the no weld access hole detail (NWAH type).

(2)The flexural strength of beam web connection of SCS, NSS, SC and NS series were strong by a thicker column flange (22mm), while that of NSW series was weak by a thinner column flange (9mm).

(3)The grade of steel of the beam of SCS, NSS and NSW series were SN490, while that of SC and NS series were SN400.

2.1.1. Welding details

The weld access hole recommended in AIJ JASS 6 (2007) is shown in Fig. 2.3. The shape of weld access hole is similar to a conventional access hole commonly used in Japan whose toe is modified to have a 10 mm radius intended to reduce the stress concentration. While the no weld access hole details recommended in AIJ JASS 6 (2007) is also shown in Fig. 2.4.

Table 2.1. Parameters of Tests and Specimens

Name of Series	Weld Access Hole	Flexural Strength	Grade of Steel	Number of Tests
SCS	JASS 6 2007	strong	SN490B	4
NSS	no weld access hole	strong	SN490B	8
NSW	no weld access hole	weak	SN490B	8
SC	JASS 6 2007	strong	SN400B	4
NS	no weld access hole	strong	SN400B	4

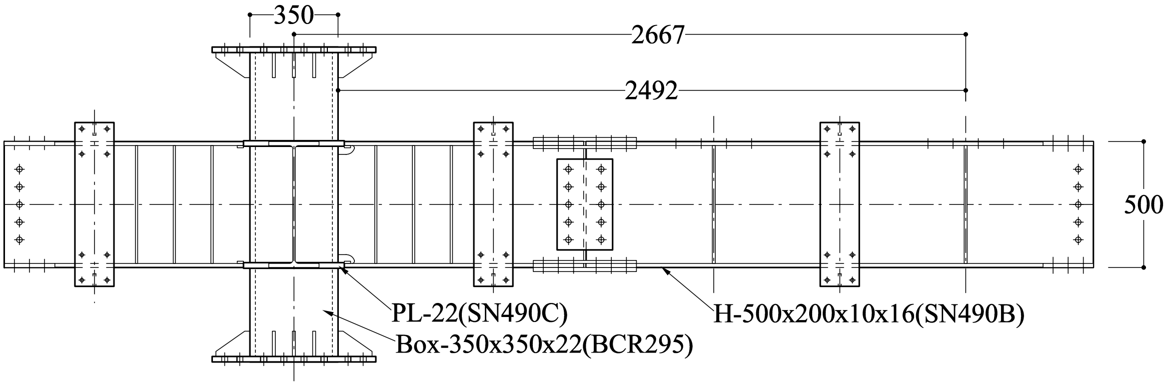

Figure 2.1. Test specimen of SN490 series (unit : mm)

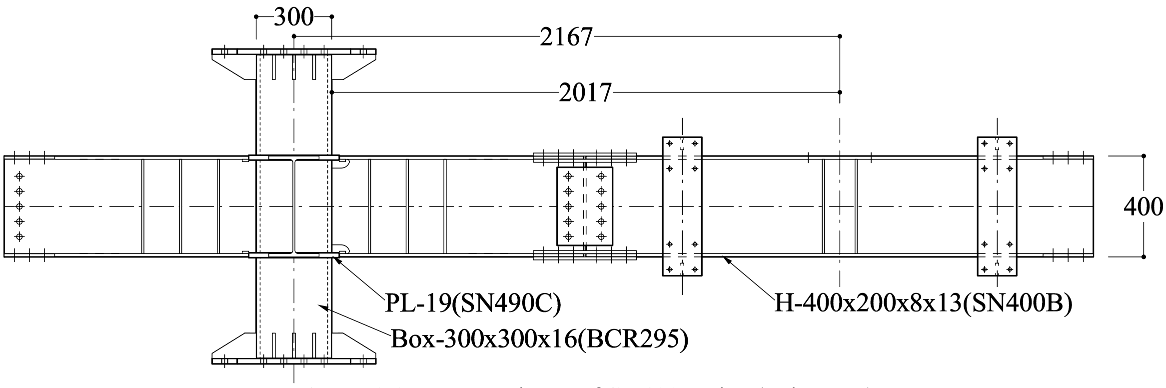

Figure 2.2. Test specimen of SN400 series (unit : mm)

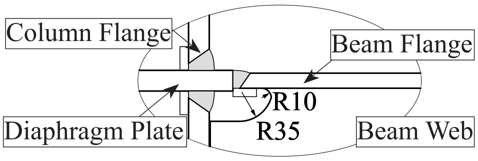

Figure 2.3. Weld access hole detail (WAH)

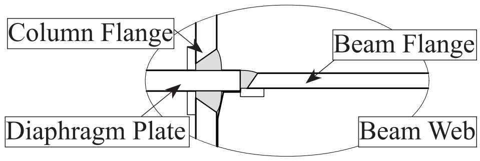

Figure 2.4. Non weld access hole detail (NWAH)

2.1.2. Flexural strength details

The evaluation of the flexural strength of beam web joint connected to a square tube column considering the out-of-plane deformation of column flange was suggested by K.Suita and T.Tanaka (2000). According to their suggestion, the ultimate flexural strength is obtained by applying the yield line theory to a combination of the collapse mechanisms of the column flange and the beam web end. Plastic deformation is only occurred at the outer edges of the beam web, not around the neutral axis. And the maximum moment expected at the beam flange. The ultimate flexural strength of beam flange ${}_jM_{fu}$ and that of beam web ${}_jM_{wu}$ are estimated as follows.

$$ {}_jM_{fu} = {}_bA_f\,({}_bd - {}_bt_f)\,{}_b\sigma_{fu} \tag{2.1}$$

$$ {}_jM_{wu} = m\ {}_bM_{wp} \tag{2.2}$$

$$ m = \min\left\{1,\ 4\frac{{}_ct_f}{{}_jd}\sqrt{\frac{{}_jb\cdot{}_c\sigma_y}{{}_bt_w\cdot{}_b\sigma_{wy}}}\right\} \tag{2.3}$$

where ${}_bA_f$ is beam flange section area, ${}_bd$ is beam depth, ${}_bt_f$ is beam flange thickness, ${}_b\sigma_{fu}$ is tensile strength of beam flange and ${}_bM_{wp}$ is the full-plastic moment of beam web. And m is the ratio of ${}_jM_{wu}$ to ${}_bM_{wp}$, which is estimated by beam web thickness ${}_bt_f$ and column flange thickness ${}_ct_f$, aspect of collapse mechanism of column flange ${}_jb$ and ${}_jd$, and the yield stress of column ${}_c\sigma_y$ and that of beam web ${}_b\sigma_{wy}$. The results of these estimations are summarized in Table 2.2. m of SCS and SC series is smaller than that of NSS and NS by the loss of section area while that of NSW series is much smaller than that of others by small thickness of column flange.

2.1.3. Grade of steel and beam section

Grade of steel of beam of SCS, NSS and NSW series are SN490 (nominal tensile strength is 490MPa and nominal yield stress is 325MPa), and that of SC and NS series are SN400 (nominal tensile strength is 400MPa and nominal yield stress is 235MPa). Beam section of SCS, NSS and NSW series are H-500x200x10x16, and that of SC and NS series are H-400x200x8x13. In conjunction with these beam sections, column sections are determined in order to keep the column and the panel zone in the elastic range even after the beam reaches full-plastic moment. The yield moment M_y and full-plastic moment M_p of all series are summarized in Table 2.3.

2.2. Test Program

2.2.1 Test setup

Loading setup of the test apparatus is as shown in Fig. 2.5. The column ends were fastened to pin supports, and two sets of lateral supports were placed to restrict out-of-plane deformation of the beam. Additionally, stiffeners were placed near the moment connection of the beam to restrict local buckling of the flange and the web. The actuator were clamped at the beam end.

Table 2.2. Ultimate Flexural Strength of Moment Connection for Each Series

Series	m	${}_jM_{fu}$ [kN·m]	${}_jM_{wu}$ [kN·m]	${}_jM_u$ [kN·m]
SCS	0.831	819	155	974
NSS	1.00	819	214	1033
NSW	0.473	819	101	920
SC	0.787	424	63	487
NS	1.00	424	95	519

Table 2.3. Sections and Strengths of Members

Series	Beam			Column			Panel	
	Section [mm]	M_y [kN·m]	M_p [kN·m]	Section [mm]	M_y [kN·m]	M_p [kN·m]	M_y [kN·m]	M_p [kN·m]
SCS, NSS, NSW	H-500x200x10x16	632	740	Box-350x350x22	987	1210	1350	1520
SC, NS	H-400x200x8x13	329	374	Box-300x300x16	583	699	697	784

2.2.2 Loading Plans

Each specimen was prepared for a constant amplitude cyclic loading test to investigate deformation capacity of the welded moment connection until ductile fracture of CJP groove welds. The constant amplitudes of cyclic loading test were 1.2θ_p, 2.0θ_p, 3.0θ_p or 4.0θ_p, where θ_p is the calculated elastic component of beam rotation corresponding to the full-plastic moment of beam at the face of the column. The component of beam rotation only was calculated using displacements measured at various locations of the test specimen. The number of specimens prepared for each amplitude was one for SCS series and two for NSS and NSW series. The number of specimens were two for 1.2θ_p amplitude and one for 2.0θ_p and 3.0θ_p amplitude respectively one for SC and NS series. The names of tests are summarized in Table 2.4.

3. EXPERIMENTAL RESULTS

3.1. Global Behavior

3.1.1. Loading history

Relationship between moment and rotation of beam obtained from the tests of SCS and NSS series by each amplitudes, and NSW, SC and NS series by 2.0θ_p amplitude are shown in Fig. 3.1. The moment reached the maximum after a few cycle of loading. After the strength decreased gradually specimens fractured. The specimens loaded by smaller amplitude fractured after the strength decreased below the 90% of the maximum strength, while specimens loaded by larger amplitude fractured before the strength decreased 90% of the maximum strength.

3.1.2. Fracture appearance

For WAH type, cracks initiated from two places, i.e. from the toe of the weld access hole and from the end of the weld line of the beam flange. The crack initiated from the toe of the weld access hole penetrated the beam flange through the thickness and resulted in fracture of beam flange. While for NWAH type, crack initiated from the end of the weld line and propagated along weld line at the bond of the beam flange side until total fracture. The fracture of beam flange weld of 2.0θ_p for SCS and NSS series are shown in Fig. 3.2.

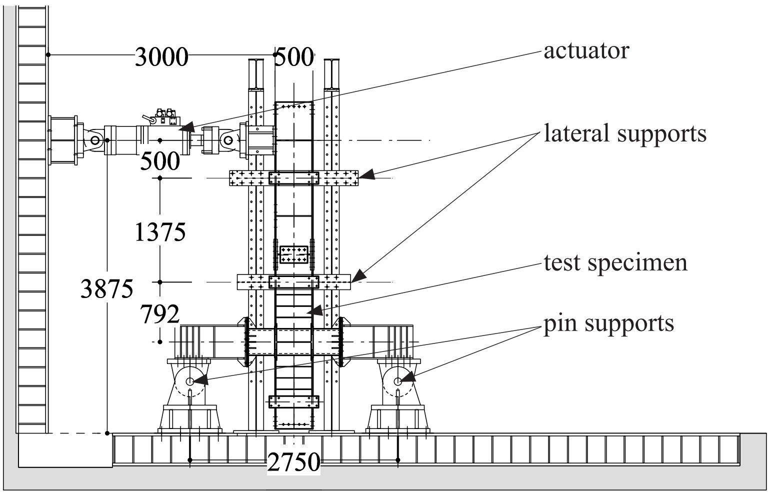

Figure 2.5. Test setup (unit : mm)

Table 2.4. Name of Tests

Amplitude	SCS series	NSS series	NSW series	SC series	NS series
1.2θ_p	SCS-1.2	NSS-1.2A,B	NSW-1.2A,B	SC-1.2A,B	NS-1.2A,B
2.0θ_p	SCS-2.0	NSS-2.0A,B	NSW-2.0A,B	SC-2.0	NS-2.0
3.0θ_p	SCS-3.0	NSS-3.0A,B	NSW-3.0A,B	SC-3.0	NS-3.0
4.0θ_p	SCS-4.0	NSS-4.0A,B	NSW-4.0A,B	-	-

3.2. Maximum Strength and Number of Cycles

Peak strength normalized by ${}_bM_p$, number of cycles and cumulative plastic deformation at the ultimate state and the fracture are summarized in Table 4.1. The ultimate state was defined as the point when the beam flange fractured or the strength was reduced to 90% of the maximum strength. In this study, cumulative plastic deformation is estimated as following equation.

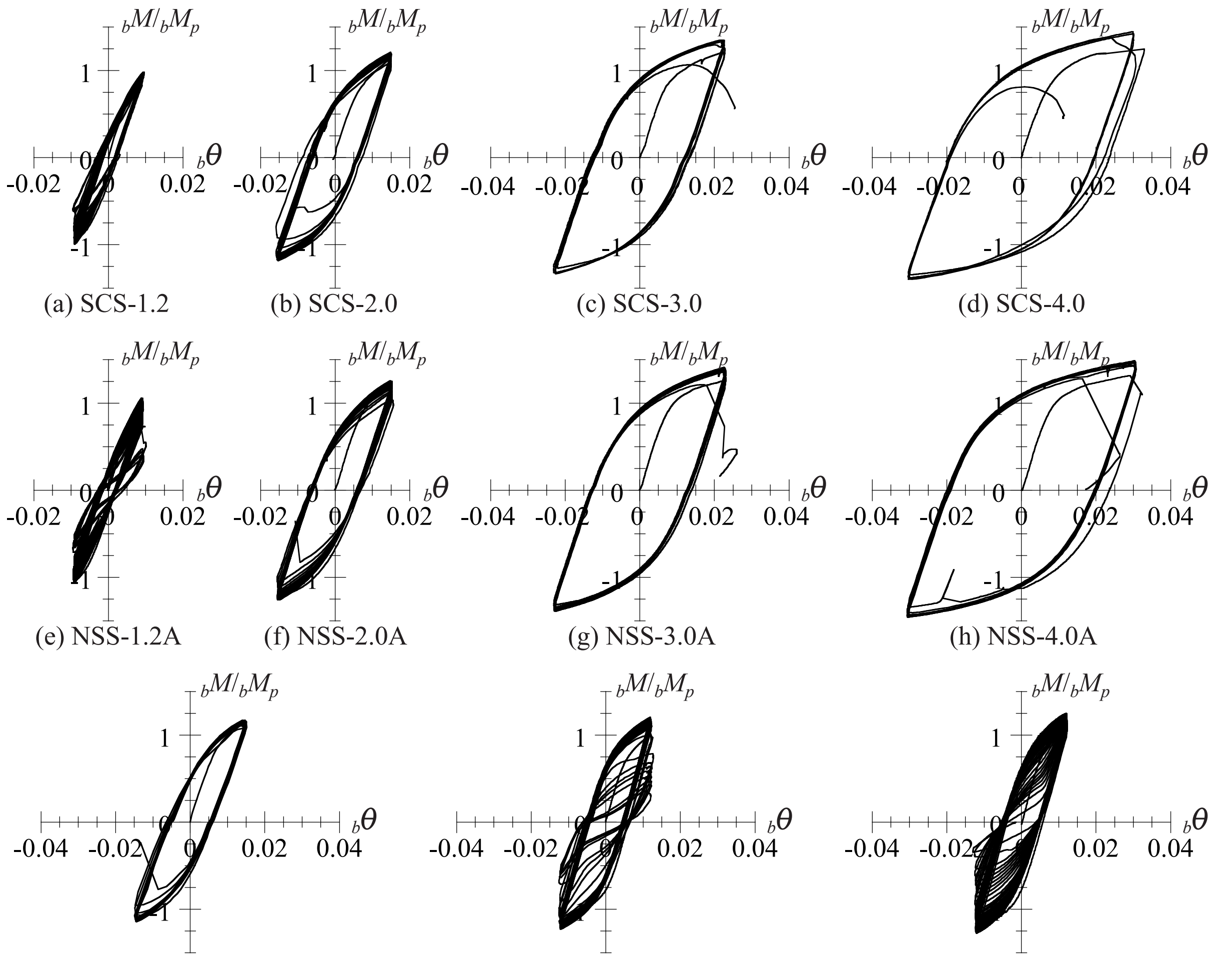

(a) SCS-1.2 (b) SCS-2.0 (c) SCS-3.0 (d) SCS-4.0

(e) NSS-1.2A (f) NSS-2.0A (g) NSS-3.0A (h) NSS-4.0A

(i) NSW-2.0A (j) SC-2.0 (k) NS-2.0

Figure 3.1. Example of moment versus rotation relationships obtained from tests

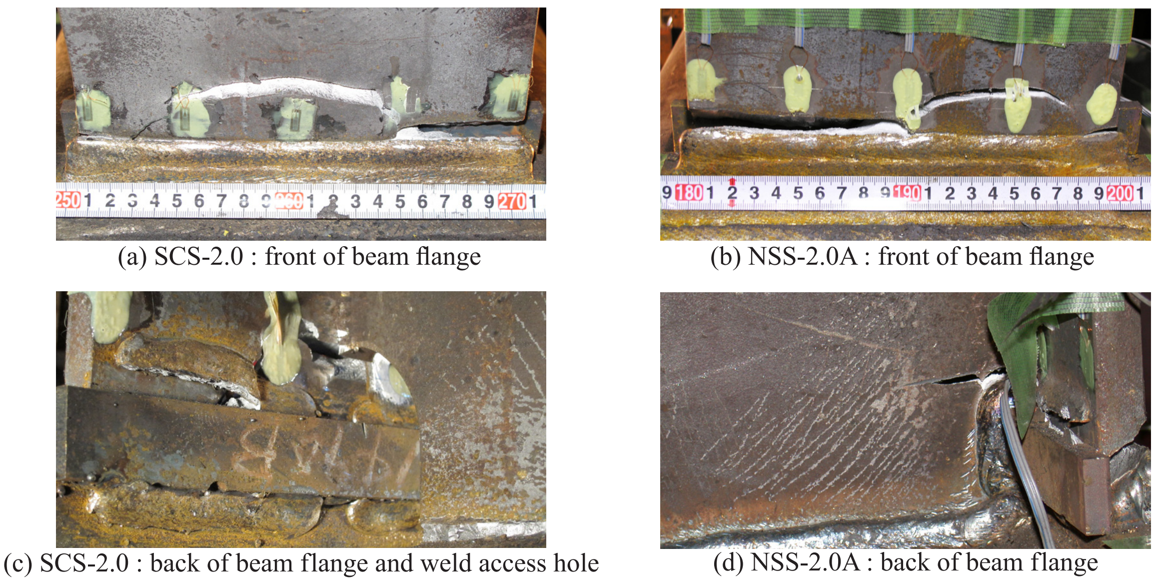

(a) SCS-2.0 : front of beam flange (b) NSS-2.0A : front of beam flange

(c) SCS-2.0 : back of beam flange and weld access hole (d) NSS-2.0A : back of beam flange

Figure 3.2. Fracture of beam flange CJP weld after tests

$$\eta = \Sigma\theta_{pi} / \theta_p \tag{3.1}$$

where θ_{pi} is plastic component of the rotation of beam at the i th cycle.

4. DISCUSSION

4.1. Deformation Capacity of Beams

The number of cycles at the ultimate state N_U and the cumulative plastic deformation until ultimate state η_U are shown in Fig. 4.1 and 4.2 by double logarithmic plot. The linear relationship is found between ductility of amplitude μ and N_U or η_U. The larger amplitude specimens have smaller deformation capacity in each series. From the comparison among specimen series, WAH type has smaller deformation capacity than NWAH type in each grade of steel. Further more, WAH type has least deformation capacity in SN490 steel.

4.2. Crack Propagation

4.2.1. Crack appearance

For WAH type, the crack initiated from the toe of the weld access hole of the beam end connection and propagated to the beam flange. The propagation of the crack is measured by crack depth D. For

Table 4.1. Test results

Name of Tests	Strength ${}_bM^{peak}/{}_bM_p$		Number of Cycles		Cumulative Plastic Deformation	
	max	min	N_U	N_F	η_U	η_F
SCS-1.2	0.98	-0.99	89	100	66	78
SCS-2.0	1.21	-1.18	31	33	96	106
SCS-3.0	1.35	-1.34	6	7	38	42
SCS-4.0	1.45	-1.40	4	5	40	44
NSS-1.2A	1.06	-1.06	235	274	207	248
NSS-1.2B	1.05	-1.04	198	225	158	186
NSS-2.0A	1.26	-1.26	61	63	186	196
NSS-2.0B	1.24	-1.23	52	55	153	163
NSS-3.0A	1.41	-1.39	25	25	155	155
NSS-3.0B	1.40	-1.35	20	20	123	123
NSS-4.0A	1.48	-1.46	13	13	127	127
NSS-4.0B	1.48	-1.45	14	14	126	126
NSW-1.2A	0.97	-0.98	205	220	171	185
NSW-1.2B	1.02	-0.98	193	280	164	301
NSW-2.0A	1.17	-1.14	36	37	108	111
NSW-2.0B	1.20	-1.17	26	28	76	81
NSW-3.0A	1.29	-1.31	14	15	88	88
NSW-3.0B	1.31	-1.30	17	17	98	98
NSW-4.0A	1.39	-1.36	7	7	63	63
NSW-4.0B	1.38	-1.37	6	6	52	52
SC-1.2A	0.99	-1.03	202	241	151	195
SC-1.2B	0.99	-1.01	262	302	225	272
SC-2.0	1.22	-1.23	58	66	171	200
SC-3.0	1.35	-1.34	17	20	112	135
NS-1.2A	1.05	-1.07	470	541	270	336
NS-1.2B	1.04	-1.07	485	635	345	481
NS-2.0	1.25	-1.28	84	101	249	305
NS-3.0	1.39	-1.39	45	49	288	317

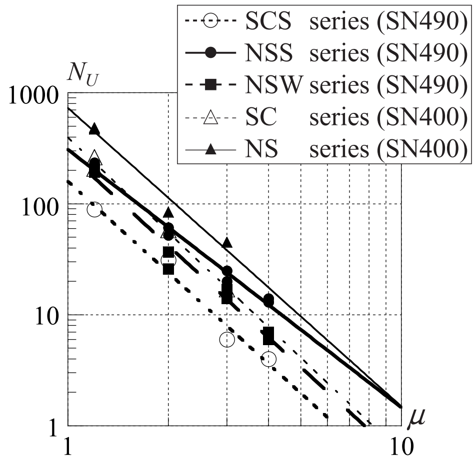

Figure 4.1. μ versus N_U relationship

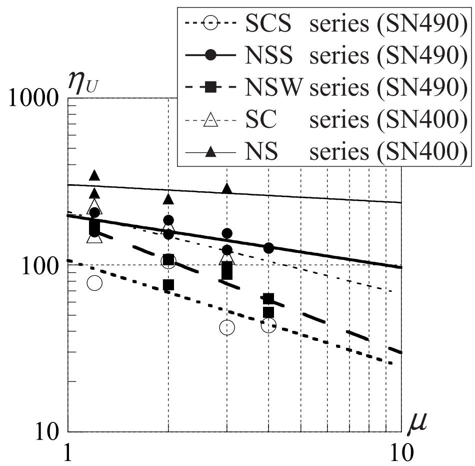

Figure 4.2. μ versus η_U relationship

NWAH type, the crack initiated from the end of the CJP weld of the beam flange and propagated along weld line. The propagation of the crack is measured by crack length L. These cracks are shown in Fig. 4.3 However, since the crack propagation of SC series did not measured after penetration of the beam flange, this crack is analyzed until the penetration of the flange, not until fracture.

All cracks propagated in three stages, i.e. firstly no cracks, secondly the cracks propagate gradually, and thirdly the cracks propagate rapidly to fracture. The relationships between number of cycles at the ultimate state N_U and at the end of the second stage N_g is shown in Fig. 4.4, and the relationships between N_U and number of cycle at the crack penetration of the beam flange N_{sc} for WAH type is shown in Fig. 4.5. These figures show that the ultimate state corresponds to the end of second stage for both WAH type and NWAH type, and at this instance, the crack initiated from the toe of the weld access hole penetrated until the face of the beam flange for WAH type. The crack propagations of all tests are shown in Fig. 4.6, whose abscissas are the number of cycles N divided by N_{sc} for WAH type and divided by N_g for NWAH type.

4.2.2. Formulation of crack propagation

In order to evaluate deformation capacity, damage to the beam flange is quantified by crack propagations which lead to fracture of welded connection. Here, the crack propagations obtained from tests are formulated to investigate the effect of parameters of tests and deformation amplitudes.

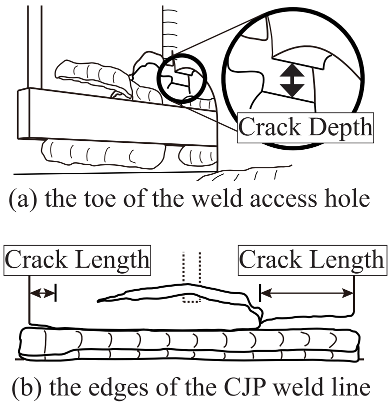

Figure 4.3. Measure points of cracks

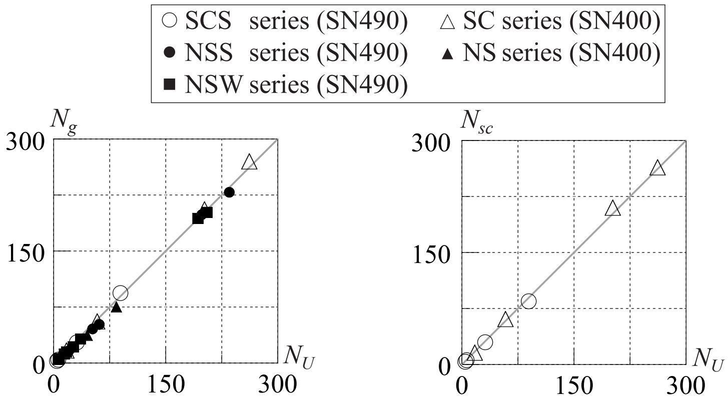

Figure 4.4. N_U versus N_g relationship **Figure 4.5.** N_U versus N_{sc} relationship

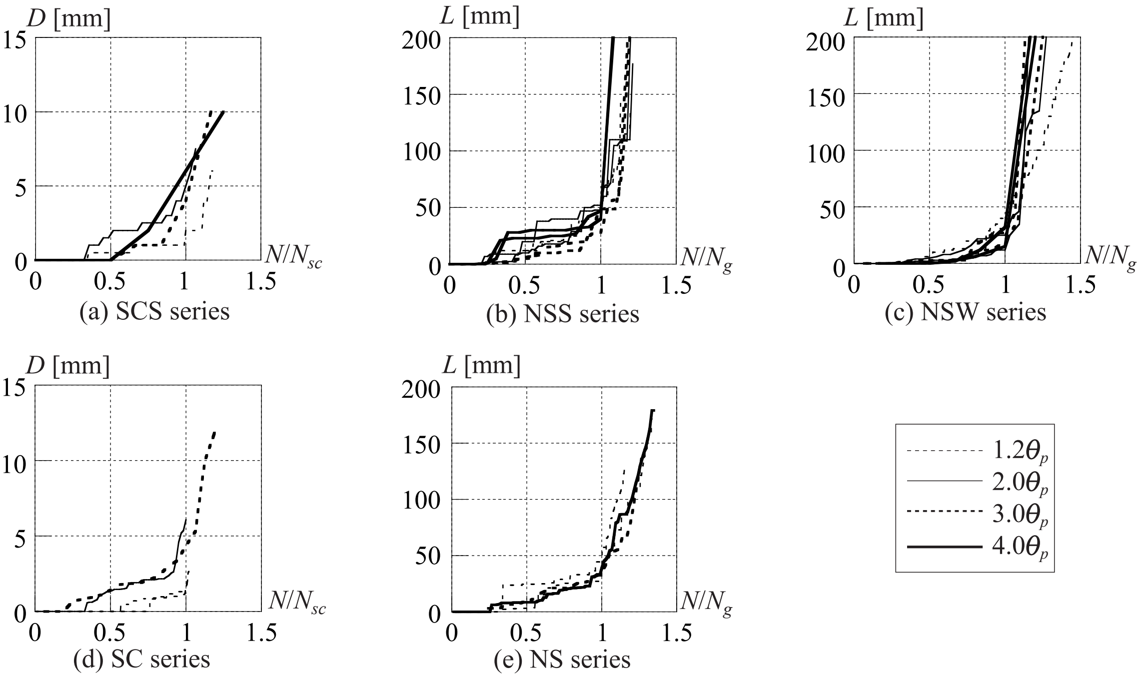

Figure 4.6. Crack propagations obtained from loading tests

Velocities of the crack propagations are calculated. Since cracks did not propagate smoothly, the smoothing of the relation between crack length or depth and number of cycles are conducted. The velocities of crack propagation are modeled as shown in Fig. 4.7, and are formulated as follows.

$$n < n_s \quad : v_1 = 0 \tag{4.1}$$
$$n_s < n < 1.0 \quad : v_2 = a_2\,(n - n_s) \tag{4.2}$$
$$n < 1.0 \quad : v_3 = a_3\,(n - 1.0) + a_2\,(1.0 - n_s) \tag{4.3}$$

where n_s is the number of cycle at the end of first stage N_s divided by N_{sc} or N_g, a_2 and a_3 are the coefficients which mean the rate of change of v_2 and v_3. Next, liner relationship between a_2 and (μ - 1.0) and between a_3 and (μ - 1.0) are obtained by regression analysis of test results. n_s is regarded as constant value regardless of μ. Test results of these coefficients are shown in Fig. 4.8 and those are summarized in Table 4.2. The coefficients a_2 and a_3 of SN490 steel beam are larger than those of SN400 steel, and those of NSW series are largest in NWAH type. n_s of WAH type is larger than that of NWAH type except NSW series. However, a_2 of NSW-4.0A is excepted from regression analysis to obtain the liner relationship since it is significantly larger than that of other NSW series.

The crack propagation of D and L are obtained by integrating v_2 and v_3 for each stage. The relationships between D or L and n obtained from these calculations are shown in Fig. 4.9. These formulated crack propagation curves include the effect of the amplitudes and the parameters of tests by the function of the number of cycles. Fig. 4.9 shows that the propagation curves are different from each other, which means that the damage defined by the formulated crack propagation curves dose not match the Miner rule of fatigue fracture.

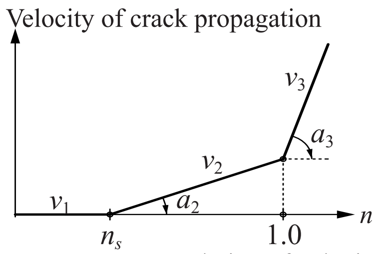

Figure 4.7. Formulation of velocity of crack propagation

Table 4.2. Results of Regression Analysis

Series	n_s	a_2	a_3
SCS	0.301	1.55(μ - 1.0)	4.87(μ - 1.0)
NSS	0.249	2.48(μ - 1.0)	551(μ - 1.0)
NSW	0.453	6.43(μ - 1.0)	312(μ - 1.0)
SC	0.481	0.455(μ - 1.0)	-
NS	0.393	1.55(μ - 1.0)	19.7(μ - 1.0)

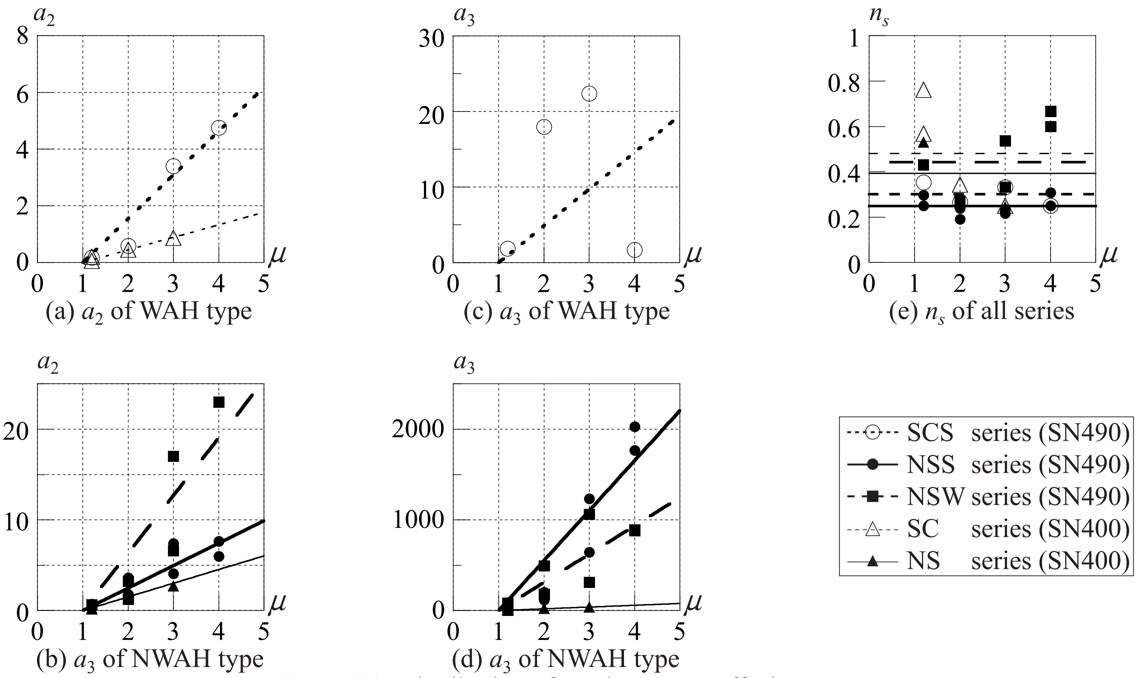

Figure 4.8. Distribution of crack curve coeffecients

4.2.3 Comparison of crack propagation

The effect of parameters of tests is investigated by comparison of formulated crack propagation curves. The propagation curves must be normalized to compare each other since the cracks for NWAH type are different from those for WAH type in measuring method. The propagation curves are divided by the crack depth at n=1.0 D_U for WAH type and divided by the crack length at n=1.0 L_U. The propagation curves of all tests after propagating cracks are shown in Fig. 4.10, whose abscissas is the number of cycles and whose ordinate is D/D_U for WAH type or L/L_U for NWAH type.

Since the relationship of the number of cycle at D/D_U=1.0 or L/L_U=1.0 as shown in Fig. 4.10 is correspond to the relationships shown in Fig. 4.1 and Fig. 4.2, these propagation curves also show the relationships of deformation capacity. Fig. 4.10 shows that the curves of specimens which have smaller deformation capacity propagate rapidly, and that the curves of specimens which have smaller deformation capacity (i.e. SCS and NSW series) are close to each other and apart from that curves of larger deformation capacity (i.e. NSS series).

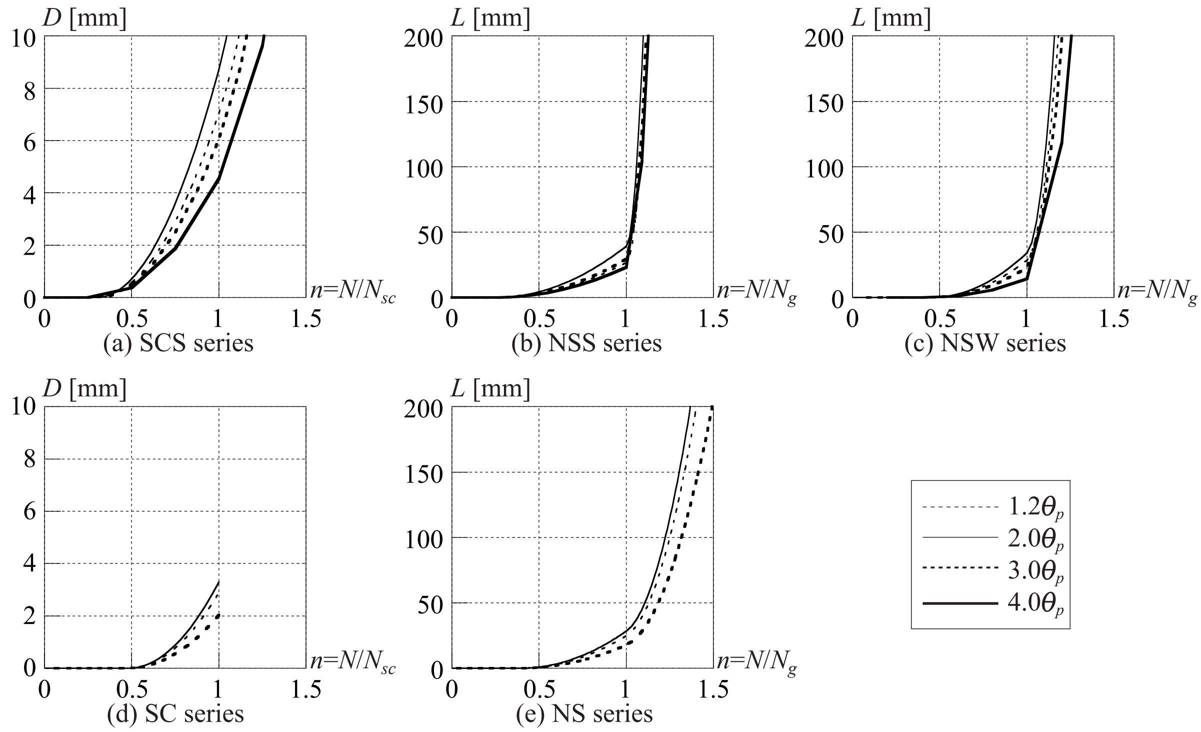

Figure 4.9. Formulated crack propagation curves of all series

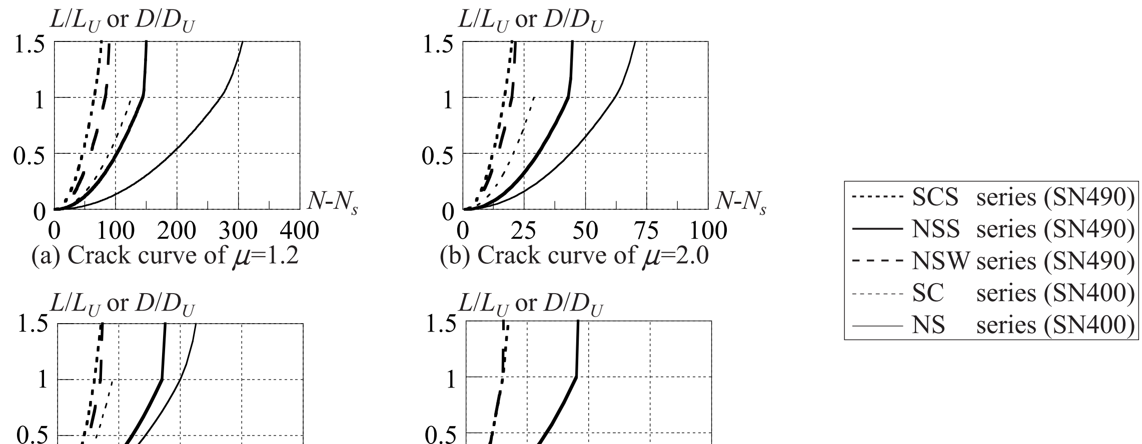

Figure 4.10. Comparison of crack curve after crack propagation

5. CONCLUSION

The steel beam-to-column subassemblages were prepared for constant amplitude cyclic loading test to investigate the effect of weld access hole details, flexural strength of beam end connection and grade of steel on deformation capacity of welded moment connections. The obtained results are as follows.
1) The liner relationship is found between the number of cycle and the cumulative plastic deformation at the ultimate state and ductility of amplitude by double logarithmic plot. The larger amplitude specimens have smaller deformation capacity, and WAH type has smaller deformation capacity than NWAH type in each grade of steel. Further more, WAH type has the least deformation capacity in SN490 steel.
2) The cracks initiated at the toe of the weld access hole for WAH type and at the end of CJP weld line of beam flange for NWAH type. The limit of deformation capacity defined by crack propagations corresponds to the ultimate state defined by hysteresis loops of the relationships between moment and rotation of beam, and that corresponds to the point when crack penetrate the beam flange for WAH type. The numbers of cycles at these points are regarded as the limit of deformation capacity.
3) In order to evaluate deformation capacity, the relationship between the crack propagation behaviour which lead to fracture of welded connection and number of cycles is calculated by regression analysis. From the formulated crack propagation curves, they are different from each other, which means that the damage defined by the propagation curves dose not match the Miner rule of fatigue fracture. Comparison of the propagation curves show that the cracks of specimens which have smaller deformation capacity propagate rapidly and the propagation curves of them are close to each other and apart from curves of larger deformation capacity.

REFERENCES

K.Suita, Y.Kitamura, T.Goto, T.Iwata, K.Kamae : Seismic response of high-rise buildings constructed in 1970's subjected to long-period ground motions (using predicted ground motions from hypothetical Nankai trough earthquakes in Kansai area), J. Struct. Constr. Eng., AIJ, No. 611, pp. 56-61, Jan., 2007

S.Yamada, Y.Kitamura, K.Suita, M.Nakashima : Experimental investigation on deformation capacity of beam-to-column connections in early highrise buildings by fullscale tests, J. Struct. Constr. Eng., AIJ., Vol. 73, No. 623, pp. 119-126, Jan., 2008

K.Suita, Y.Kitamura, I.Hashida : Seismic performance and retrofit of beam-to-column connection for early high-rise buildings, J. Struct. Constr. Eng., AIJ., No. 74, Vol. 636, pp. 367-374, Feb., 2009

K.Inoue, T.Kamba, et.al. : full-scale test on plastic rotation capacity of steel wide-flange beams connected with square tube steel columns (Part 1 ~ Part 5), Steel Constr. Eng., JSSC, Vol. 4, No. 16, Dec., 1997

T.Fujita, T.Nakagomi : Mechanical behaveor of rolled H-shaped steel beam connected to square-shaped steel pipe column with through diaphragms (effect of scallops and unevenness on fracture), J. Struct. Constr. Eng., AIJ, No. 455, pp. 187-196, Jan., 1994

H.Kuwamura, N.Takagi : Similitude low of prefracture hysteresis of steel moment, J. Struct. Eng., ASCE, pp. 752-761, May 2004

J.Iyama, J. M. Ricles : Prediction of fatigue life of welded beam-to-column connections under earthquake loading, J. Struct. Eng., ASCE, pp. 1472-1480, Dec. 2009

K.Suita, T.Tanaka, A.Sato, Y.Manabe, T.Tsukada, Z.Su : Effect of ultimate flexural strength of beam end connection on deformation capacity (deformation capacity of welded beam-to-column connection subjected to repeated plastic strain part 1), J. Struct. Constr. Eng., AIJ, Vol. 76, No. 664, pp. 1135-1142, Jun., 2011

D. K. Miller : Lessons learned from the Northridge earthquake, Eng. Struct., Vol. 20, Nos 4-6, pp.249-260, 1998

Federal Emergency Management Agency : Recommended seismic design criteria for new steel moment-frame buildings, FEMA-350, Jul. 2000

AIJ : Japanese architectural standard specification JASS 6 Steel Work

AIJ : Recommendation for design of connections in steel structures, second edition, 2006

K.Suita, T.Tanaka : Flexural strength of beam web to square tube column joints, Steel Constr. Eng., JSSC, Vol. 7, No. 26, Jun., 2000

K.Takatsuka, Y.Manabe, K.Suita, T.Tanaka, T.Tsukada, Z.Su : Effect of weld access hole on deformation capacity (deformation capacity of welded beam-to-column connection subjected to repeated plastic strain part 2), J. Struct. Constr. Eng., AIJ, Vol. 77, No. 673, pp. 453-459, Mar., 2012